

# ROBUST ADAPTIVE PROCESSING IN LITTORAL REGIONS WITH ENVIRONMENTAL UNCERTAINTY

LISA M. ZURK, NIGEL LEE, BRIAN TRACEY  
*244 Wood St., Lexington, MA 02420, zurk@ll.mit.edu*

## 1 Introduction

Detection and localization of quiet targets in littoral regions presents a challenging problem both because of the complicated acoustic propagation that occurs and the prevalence of loud surface ship interference. Matched Field Processing (MFP) can help address the first concern by using a propagation model to determine the steering vectors, thus providing optimal array gain and localization accuracy. Adaptive MFP (AMFP) can provide the ability to null surface interference, particularly when an array has vertical aperture that allows discrimination of surface and submerged sources. Under ideal situations, AMFP can provide super-resolution and add 10-20 dB interference suppression.

However, performance gains from AMFP have yet to be realized in practice, for several reasons. Perhaps the most important limitation is that precise information on the underwater channel is generally not available. The mismatch between the computed and actual array steering vectors can result in loss of array gain and - for adaptive processing - significant target self-nulling. A second factor influencing the performance of AMFP is the motion of the targets and interferers which introduces additional signal loss, smearing of source peaks, and consumption of adaptive degrees of freedom.

In this paper, we begin by examining the detection and localization performance for stationary sources as a function of the beamformer. We then quantify the effects of target and interferer motion. Finally, we present two methods that address two of these loss mechanisms. The first method uses the invariance principle to compensate for target motion and decrease signal gain degradation. The second method uses the observed response from a loud source and applies a depth shifting operation to construct a steering vector at the depth of interest.

## 2 System Performance

MFP suffers signal gain degradation due to imperfect knowledge of the underwater channel. Range-focused single-path beamformers (RFBF) suffer loss due to approximation of a multipath environment as a single path one. The losses of both of these are a function of the array topology, the position of the target, and the underwater environment. For sonar systems, it is useful to understand the expected losses to determine the appropriate beamformer for the best detection performance (i.e., minimal losses) in a given target region.

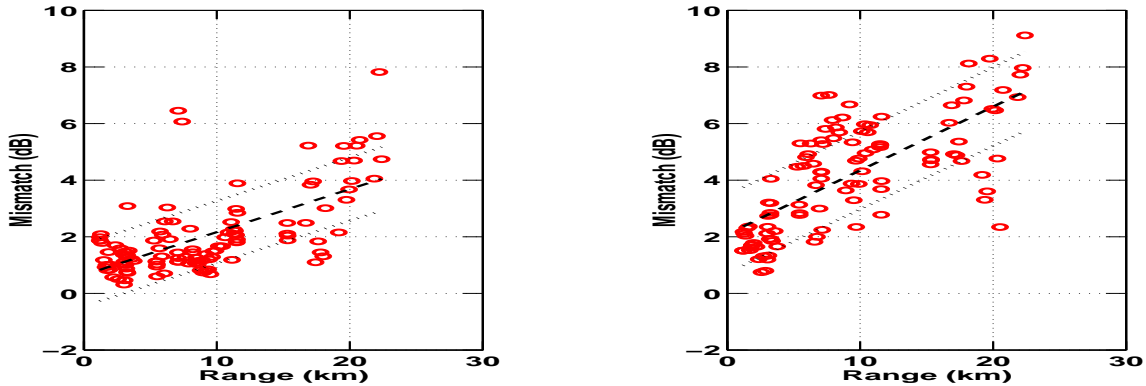


Figure 1. Mismatch from SBCX data as a function of source range for towed source tones at 94 Hz (lefthand plot) and 235 Hz (righthand plot).

Monte Carlo simulations that incorporate the expected error in the shallow water environment were used to determine MFP mismatch loss. These simulations indicate that the loss grows as a function of target range. If one models the error as a perturbation of the modal wavenumbers, it can be easily understood that the total error will accumulate as the range to the source grows. This has been verified with experimental data from the Santa Barbara Channel Experiment, which is shown in Fig 1, where the measured mismatch to a towed source are plotted for the tone at 94 Hz (left) and 235 Hz (right).

RFBF simulations show that the losses do not grow as a function of target range, implying that there is a range at which the losses from MFP exceed those of RFBF. RFBF losses are also greatest at endfire, where exposure to the unaccounted-for modal structure produces the greatest error. This is particularly true for arrays with vertical aperture, where one sees splitting of target energy into different beams (i.e., "mode splitting").

The implications of the above are that standard MFP might provide acceptable detection performance at close ranges and in endfire regions, but in other regions mismatch losses can be excessive and application of a RFBF may provide superior detection performance.

When localization performance is considered, MFP provides vastly increased localization accuracy. In the littoral region, where interferers are typically on the surface and targets of interest are submerged, the ability to determine depth (in particular) allows one to easily classify sources. This same discrimination capability allows adaptive processors to cancel interference while retaining target. Drawbacks of such fine resolution are the large number of beams required to cover an area and the susceptibility to motion losses.

MFP range and depth resolution does not depend on the array but depend on the wavelengths of the propagating modes. This is because MFP exploits the phasing between the modes to determine source position, which produces superior performance. For RFBF, the resolution is inversely dependent on the horizontal and vertical aperture, respectively. As an example, consider a 50 Hz source in a 200 m iso-speed channel. The MFP range resolution is approximately 46 m. For an array using range focusing, this resolution could only be achieved (assuming a 5 km target range) if the array had 4000 meters of horizontal aperture.

In a typical underwater environment, targets, interferers, and often the receive array are moving in time. This is problematic for adaptive beamformers which commonly estimate the covariance matrix by averaging over some observation period during which stationarity is assumed. The total observation time is dictated by the number of elements in the array and the coherent integration time. As just discussed, large arrays with many elements provide fine resolution, so a moving source will transit more beams during a given observation period. Thus, volumetric arrays have a particularly challenging motion problem, since they require a large number of snapshots, leaving them vulnerable to motion losses. Many approaches for addressing this problem have been proposed, such as reduced-dimension processing, time-varying pre-filtering of the data, and sub-aperture processing (. For moving targets, the motion spreads the target energy across multiple beams, thus decreasing the signal excess and degrading target localization accuracy. An algorithm for addressing target motion is presented in the following section.

### 3 Robust Algorithms

Many algorithms that provide robustness to either environmental mismatch or source motion have been devised. In this section we discuss two novel techniques. The first, an invariance motion compensation algorithm, exploits the approximate invariance of the modal intensities to construct a covariance matrix in which the target motion is compensated. The algorithm is an extension of model-based compensation algorithms that have been demonstrated in the past [1], [2] with the important difference that this version does not rely on environmental knowledge. The second algorithm considered uses the observed response from what will be termed a “guide source” to determine the steering vector for a given location. With knowledge of the guide source location, this vector can then be shifted in depth to provide a steering vector for beamforming to alternate depths. Thus, an accurate replica vector is obtained without the need for environmental knowledge or the use of a propagation model.

#### 3.1 Invariance Motion Compensation

As previously discussed, long observation times may be necessary for adaptive processing but can result in signal gain degradation for moving targets. The goal of the invariance motion compensation is to provide a means of constructing a covariance matrix for adaptive processing in which the target appears as a stationary source, perhaps at a position that is at the mid-point of its track during the observation time. Previous methods presented by the authors [2] accomplished this by adjusting each data snapshot according to a propagation model. While good motion compensation was demonstrated with this method, it suffered from the potential inaccuracies introduced by environmental uncertainties and it was computationally expensive. To address these shortcomings, we present here a method that compensates for motion in a computationally feasible manner and without the requirement of environmental information. The normal mode representation of the field at frequency  $\omega$  and time  $t$  that is present on a sensor at depth  $z$  due to a source at a range  $r$  and depth  $z_s$  can be written as:

$$p(z_s, z, r; \omega, t) = C \sum_{m=1}^M \psi_m(z_s) \psi_m(z) \frac{e^{i(k_m(\omega) + i\alpha_m(\omega))r(t)}}{\sqrt{k_m(\omega)r(t)}} \quad (1)$$

where  $\psi_m$  is the mode function,  $k_m$  is the horizontal wavenumber, and  $\alpha_m$  is the attenuation constant of the  $m$ th mode;  $M$  is the total number of propagating modes; and  $C$  is a constant that includes the source amplitude. In the above, we consider a small frequency range ( $\Delta\omega/\omega \leq 10\%$ ) and thus suppress the weak dependence of the mode functions on frequency. We further consider source and receiver depths that are constant over time. Using (1), the  $i, j$ th component of the time-averaged covariance matrix can be written as

$$\hat{K}_{i,j} = \frac{1}{L} \sum_{l=1}^L p(z_s, z_i, r_i; \omega, t) p^H(z_s, z_j, r_j; \omega, t) \quad (2)$$

when averaging over  $L$  snapshots. It can be seen from (1) and (2) that a source moving in range introduces a time-varying phase term of  $k_m(\omega)r_i(t_l) - k_n(\omega)r_j(t_l)$ . This phase introduces decorrelation into the estimated covariance and results in loss of signal energy. The objective of this algorithm is to choose data samples in time and frequency so that this phase remains constant over the  $L$  snapshots.

To find the stationary phase point, we utilize the invariance principle [3] which can be written in terms of a wavenumber difference  $\chi_{mn}$  as

$$\beta = \frac{r}{\omega} \frac{dr}{d\omega} = -\frac{\chi_{mn}(\omega)/\omega}{d\chi_{mn}(\omega)/d\omega}, \quad \chi_{mn}(\omega) = k_m(\omega) - k_n(\omega) \approx \chi_{mn0} \omega^{-1/\beta} \quad (3)$$

For many shallow water regions of interest, the value of beta has been shown to be approximately equal to one, and thus (3) provides a simple relation between the frequency and range variation of the pressure field. Consider first a vertical line array (VLA) so that  $r_j = r_i$  for all  $i, j$  and the time-varying phase can be written as

$$(k_m(\omega) - k_n(\omega))r(t) = \chi_{mn}(\omega)r(t) \quad (4)$$

To maintain a constant phase in (4) we want to find the frequency offset  $\Delta\omega$  that satisfies

$$\chi_{mn}(\omega_0)r(t_0) = \chi_{mn}(\omega_0 + \Delta\omega)r(t) \quad (5)$$

at all times  $t$ . The solution can be written as

$$\omega(t) = \omega_0 + \Delta\omega(t) = \omega_0 \frac{r(t)}{r(t_0)} \quad (6)$$

which represents the time-varying frequency at which to acquire data snapshots. Note that this solution requires knowledge of the time-dependent source range relative to the initial range. As this is generally not known, the algorithm can be implemented to search over motion hypotheses, where the correct track will provide optimal signal gain. The output of the processor will thus provide concurrent target detection, localization, and tracking. The search can be optimized by assuming that the motion is linear, in which cases each motion hypothesis collapses to a slope in time-frequency space along which to acquire snapshots. The motion-invariant covariance estimation can be written as:

$$\hat{K} = \frac{1}{L} \sum_t \mathbf{x}(\omega(t_l), t_l) \mathbf{x}^H(\omega(t_l), t_l) \quad (7)$$

where  $\omega(t_l)$  is given by (6). Thus, the invariance motion compensation algorithm consists of the following steps: 1) hypothesize a target motion hypothesis, 2) collect data samples

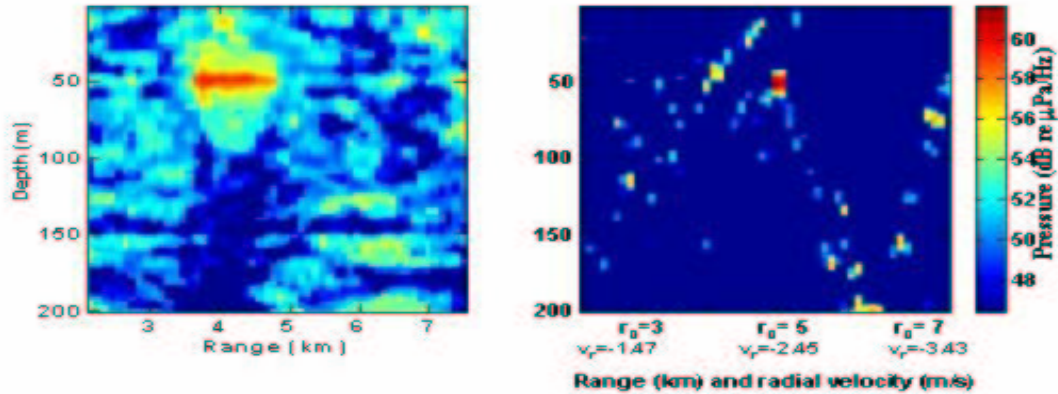


Figure 2. Range-depth ambiguity surfaces for uncompensated motion (left) and results from invariance compensation (right).

across time and frequency to construct a covariance matrix as given in (7), and 3) apply the adaptive beamformer in the standard fashion.

The result of applying motion compensation can be seen in the simulation results shown in Fig. 2. The left-hand plot shows the AMFP range-depth ambiguity plot from an incoherent average over 30 frequencies 153-183 Hz with an eight minute observation time and 8 sec coherent processing windows. The simulation was for a 50-m deep source moving 3 m/s in the 200-m Santa Barbara Channel environment with a 30-element VLA and a 60 dB white noise background. The target motion causes smearing of the peak and loss of target energy. The right-hand plot is the AMFP output for the same data when invariance motion compensation is applied. In this result, the target energy is focused at a single spatial location resulting in higher signal energy, lower noise background, and better source localization.

For a horizontal line array (HLA), the range appearing in the phase term is element dependent. The compensation algorithm then includes pre-multiplying each snapshot by a frequency dependent phase adjustment. This introduces one additional computational step and also necessitates knowing the mean wavenumber at each frequency.

The invariance motion compensation algorithm presented here provides a method for correcting for target motion in a computationally efficient manner and without requiring environmental information for the compensation. This correction produces a stationary covariance matrix which can then be used for adaptive processing. One factor worth noting is that the compensation is "tuned" for a given source motion. Additional sources with different motion characteristics will not be compensated for and will be de-focused from the process. For sufficiently long observation intervals (which is the situation this algorithm is intended for) this de-focusing can serve to decrease interferer energy in any one beam.

### 3.2 Depth Shifting of a Guide Source

In many situations of interest, strong acoustic sources are present in the environment and their locations are known. Some of these could be sources of opportunity such as surface ships, whose position might be obtained from an off-board sensor or from an airborne surveillance platform. We will term these loud sources as *guide sources* since they can be used to determine the acoustic response across a given array. This response is immediately known for the source-receiver path of the guide source, but it is still unknown for sources at alternate locations. One approach to address this is to use the response from the guide source and invert for the geophysical parameters that describe the environment (sound speed, sediment densities, etc.). This approach has been investigated with some success in the underwater community, but it suffers from the large number of ambiguities and the computational complexity of the inversion.

The alternate approach presented here instead attempts to determine the response of a source by translating the observed response from the guide source. In an ideal case, this translation would be independent of the environment and hence would not necessitate environmental knowledge. In previous work [4], translation of a response from one source range to another was demonstrated by utilizing multi-frequency data and the invariance principle described above. However, if the guide is a surface ship and the target of interest is a submerged source, a method of translating in depth (as opposed to range) is desired. In this section a method of "depth shifting" the guide source response using a fully-spanning VLA is presented.

For a VLA, output from a conventional matched field processor can be written as

$$I(z_s, r) = |\mathbf{w}^H(z_s, r) \cdot \mathbf{x}(z_s, r)|^2 \quad (8)$$

where  $\mathbf{x}(z_s, r)$  is the received data from a source at depth  $z_s$  and range  $r$ . For a conventional processor,  $\mathbf{w}(z_s, r)$  is the normalized replica vector computed at the same range and depth. For depth shifting, the weight vector is instead a translated version of a data observation from the guide source. For a guide at depth  $z_g$  and range  $r_g$ , it can be written as

$$\begin{aligned} \mathbf{w}^H(z_s, r) &= \bar{A}(z_s, r, z_g, r_g) \mathbf{x}(z_g, r_g) \\ A_{i,j} &= i - j \quad \text{for } i = j \pm 1 \quad \text{or } 0 \text{ otherwise} \end{aligned} \quad (9)$$

In the following, we briefly motivate the above choice of the translation matrix  $\bar{A}$  whose form computes a centered finite difference in the depth dimension. The depth dependence in (1) is contained in the mode functions, which are a function of both the horizontal modal wavenumber and source depth. If we make the assumption that the dependence is on the *product* of the two, we can consider  $\Psi_m(z)$  as a function of the form  $f(k_m z)$  and write

$$\begin{aligned} \frac{d}{dz} f(k_m z) &= g(k_m z) \left[ k_m + \frac{dk_m}{dz} z \right] \sim g(k_m z) k_m \quad (10) \\ \frac{d}{dk_m} f(k_m z) &= g(k_m z) z = \frac{d}{dz} f(k_m z) \frac{z}{k_m} \sim \frac{(f(k_{m+1}, z) - f(k_{m-1}, z))}{(k_{m+1} - k_{m-1})} \frac{z}{k_m} \end{aligned}$$

where the last equation follows from a centered finite difference approximation. If we then apply the mode orthogonality condition and assume that the horizontal wavenumbers have a linear dependence on mode number at small vertical angles, we arrive at the discrete

version of a new (but approximate) orthogonality expression for the mode functions:

$$\sum_0^D \frac{d}{dz} f(k_l z) f(k_m z) z dz = \frac{1}{2} [\delta(m-l-1) - \delta(l-m-1)] l \quad (11)$$

The above equation suggests that the inner product between the pressure across a VLA and the discrete difference of these pressures will produce a Dirac delta function between neighboring modes. The implications of this can be seen by writing  $I(z_s, r)$  with  $\bar{w}(z_s, r)$  given by (10) and using (11) to arrive at

$$I(z_s, r) = \left| \sum_m^M \Psi_m(z_s) \Psi_m(z_g) e^{i(k_m r - k_{m+1} r_g)} - m \Psi_{m+1}(z_s) \Psi_m(z_g) e^{i(k_{m+1} r - k_m r_g)} \right|^2 \quad (12)$$

This differs from the conventional MFP expression because the quantity is evaluated at mode indices  $m$  and  $m+1$  (the conventional expression contains only the index  $m$  for a fully-spanning VLA). Thus, the maximum output does not occur when  $z_g = z_s$  and  $r_g = r$ , but for some other “shifted” location. As an example, if we use the analytic expressions for an isospeed waveguide we can show that (for  $r = r_g$ ) the maximal output occurs when

$$z_s \sim z_g \pm \frac{\pi}{Dk_0} r = z_g \pm \frac{c}{2fD} r \quad (13)$$

This relationship is illustrated in Fig 3 where the MFP output  $I(z_s, r)$  is shown for a 235 Hz simulation in the Santa Barbara Channel environment with  $r_g = r = 2.5$  km. The output is plotted as a function of the guide source depth and the target depth,  $z_g$  and  $z_s$ , respectively. If conventional processing had been applied, the plot would have high energy only along the diagonal where the guide and target depths are equal. In contrast, for the depth-shifted output, the high energy occurs along the ridges defined by  $z_s = z_g \pm 40$ . This value is the solution obtained from (13), even though the environment is not an isospeed channel (it has a downward refracting water column, with two sediment layers). This suggests that the relationship between the guide depth and the shifted depth may be only weakly sensitive to details of the environment.

The right-hand plot in Fig 3 is the same simulation but with a 20% steeper sound speed profile, a faster bottom layer, and an additional sediment layer. Although some of the power has dissipated, the result shows the same general peak structure, as did simulation results for an isospeed and Pekeris waveguide (not shown).

The above algorithm provides a method of using a known response (e.g. steering vector) from one depth and translating it to another depth by utilizing a VLA. It relies on a new mode orthogonality relationship which shifts the modes that contribute to the MFP output. Initial investigation of this relationship indicate it is insensitive to the fine features of the environment, but further examination is required. For arrays that do not have sufficient vertical aperture, there may be alternate methods of accomplishing the mode shift and the resultant depth shift.

## 4 Conclusion

Standard Matched Field Processors hold the promise of increased target gain and localization accuracy, but their performance is strongly dependent on fine knowledge of the

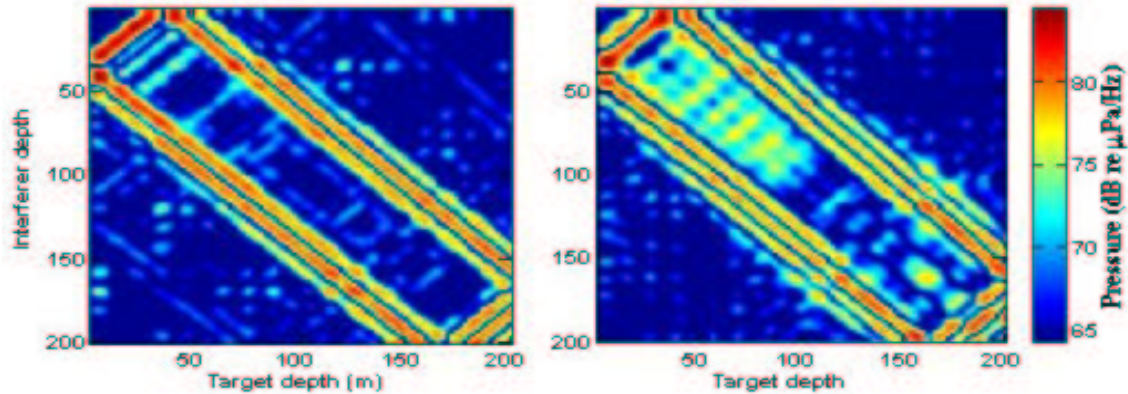


Figure 3. MFP output from depth-shifting guide source algorithm.

underwater environment. In this work, two methods of providing robustness are presented. Invariance motion compensation utilizes the invariance principle to compensate for target motion in a robust and computationally feasible method. The depth shifting algorithm utilizes a new, approximate mode orthogonality relationship to translate the response from a known guide source for beamforming to alternate target locations.

### Acknowledgements

This work was sponsored by DARPA-ATO under Air Force contract F19628-01-C-0002. Opinions, interpretations, conclusions, and recommendations are those of the authors and are not necessarily endorsed by the Department of Defense.

### References

1. Zurk, L.M., Lee, N. and Ward, J., Adaptive Matched Field Processing of Moving Sources in the Santa Barbara Channel Experiment, submitted to Jour. Acoust. Soc. Am., June 2001
2. Zurk, L.M., Lee, N. and Ward, J., 3D Adaptive Matched Field Processing for a Moving Source in a Shallow Water Channel, IEEE Oceans '99, Seattle, WA, 3 vol. xxxiv pp.728-31 vol.2, Sept. 1999
3. L. M. Brekhovskikh and Y. P. Lysanov, Fundamentals of Ocean Acoustics, 2nd ed. (Springer-Verlag, Berlin, 1991), pp. 139
4. H. C. Song, W. A. Kuperman, and W. S. Hodgkiss, "A time reversal mirror with variable range focusing," J. Acoust. Soc. Am. 103, 3234(1998).